Journal of Power Sources 195 (2010) 3536–3545

Contents lists available at ScienceDirect

Journal of Power Sources

journal homepage: www.elsevier.com/locate/jpowsour

An impedance study for the anode micro-porous layer in an operating direct methanol fuel cell

Shu-Han Yang[a,*], Charn-Ying Chen[b], Wen-June Wang[a]

[a] Department of Electrical Engineering, National Central University, Jhong-li, 320, Taiwan
[b] Institute of Nuclear Energy Research (INER), Longtan, Taoyuan, 325, Taiwan

ARTICLE INFO

Article history:
Received 20 November 2009
Accepted 10 December 2009
Available online 21 December 2009

Keywords:
Gas diffusion layer (GDL)
Micro-porous layer (MPL)
Direct methanol fuel cell (DMFC)
Membrane electrode assembly (MEA)
Electrochemical impedance spectroscopy (EIS)

ABSTRACT

This study presents the benefit to an operating direct methanol fuel cell (DMFC) by coating a micro-porous layer (MPL) on the surface of anode gas diffusion layer (GDL). Taking the membrane electrode assembly (MEA) with and without the anodic MPL structure into account, the performances of the two types of MEA are evaluated by measuring the polarization curves together with the specific power density at a constant current density. Regarding the cell performances, the comparisons between the average power performances of the two different MEAs at low and high current density, various methanol concentrations and air flow rates are carried out by using the electrochemical impedance spectroscopy (EIS) technique. In contrast to conventional half cell EIS measurements, both the anode and cathode impedance spectra are measured in real-time during the discharge regime of the DMFC. As comparing each anode and cathode EIS between the two different MEAs, the influences of the anodic MPL on the anode and cathode reactions are systematically discussed and analyzed. Furthermore, the results are used to infer complete and reasonable interpretations of the combined effects caused by the anodic MPL on the full cell impedance, which correspond with the practical cell performance.

1. Introduction

The liquid feed direct methanol fuel cell (DMFC) has received much attention as a leading candidate power source for portable electronic devices and light vehicles because of its unique advantages such as high energy conversion efficiency, easy delivery and storage of liquid fuel, ambient temperature operation and simple construction [1–5]. The cell performance critically depends on the core component of the membrane electrode assembly (MEA), which consists of a polymer electrolyte membrane, the catalyst of the electrode, and gas diffusion layers. So far, investigations have elaborated on the improvement of the membrane material, the increase of the active area of the catalyst and the optimal operating conditions to enhance the efficiency and performance of MEA in a DMFC system. However, the key problems of the lower electrocatalytic activity, methanol crossover and questionable long-term durability of MEA still prevent the widespread commercial application of DMFC [5].

Compared with the use of hydrogen in PEMFCs, the use of liquid methanol solution will result in more complex transport dynamic on the anode side of DMFCs. As the liquid methanol solution diffuses through the gas diffusion layer (GDL) and electro-oxidizes on the anodic catalyst surface, the product of CO_2 must be quickly removed from the active area of the catalyst surface to avoid a low efficiency of catalyst utilization [6]. Hence, the transport of CO_2 gas and aqueous methanol solution move counter currently, which causes the two phase transport in the GDL. Consequently, the physical parameters of the GDL such as the thickness, pore size and pore distribution, which affect the dynamics of two phase transport, had been researched in several literatures [6–11]. Theoretically, these flows on the anode side should be isolated such that discrete paths for gas transport and for liquid flow exist, rather than a two phase flow with gas bubbles moving against a liquid flow. To realize this ideal, the simplest way was to make the GDL surface hydrophobic, thereby creating a greater region for free gas movement. Thus, adding PTFE to the surface of the anode GDL, which was based on carbon cloth or carbon paper, had been studied [6,8–10,12–18]. However, the use of a PTFE-treated GDL would result in a lower limiting current density due to the increased mass transport resistance and ohmic losses [8–10]. To tailor mass transport properties and ohmic losses, a thin micro-porous layer (MPL), consisting of carbon power and PTFE or Nafion, was coated on the GDL surface [18–20]. The use of a MPL could reduce the voltage drop in-plane direction of electrode due to the low contact resistance and provide a barrier to methanol and water crossover [15,18,21–24]. On the anode side the structure provided more secondary pores to facilitate the gas evolution and had to ensure efficient supply of the active sites with methanol to avoid mass transfer limitations under operation

* Corresponding author. Tel.: +886 3 4227151x34562; fax: +886 3 4255830.
E-mail address: kalodolum@anet.net.tw (S.-H. Yang).

0378-7753/$ – see front matter © 2009 Elsevier B.V. All rights reserved.
doi:10.1016/j.jpowsour.2009.12.043

[18,19,25]. Nevertheless, the high level of carbon loading in the MPL possibly restricted the agglomerate diffusion on the anode side, thereby decreasing the performance of the cell [15,19,21]. Moreover, which types of the anode MPLs (hydrophobic or hydrophilic) benefit the performance of DMFCs had been investigated. The hydrophilic MPL with Nafion as binding agent yielded a smaller through-plane mass transport resistance than did the hydrophobic MPL using PTFE as the binding agent [14,18,19]. Notably, higher cell performance at high current density was observed by using PTFE as binder because PTFE bonded blacking structure provided better CO_2 removal than that of Nafion [18]. However, a negligible effect on methanol transport by using a hydrophobic MPL was reported [23]. In addition, the pore-distributions of MPL in DMFCs had been discussed [20,25–27].

However, most of the previous studies, which focus on the hydrophobic or hydrophilic degree of MPL and the distribution of pores in MPL, point out that adding anode MPL increases the mass transfer resistance, reducing the cell performance. In terms of cell principle, anode MPL is not an indispensable one; but in practice, if without anode MPL, the cell performance will be suppressed to a degree [20,23,26–28]. Then, the anode MPL is an important unit for DMFCs but the function is obscure. Moreover, the influences of anode MPL on DMFCs are mostly evaluated by the electrochemical impedance spectroscopy (EIS) during the half cell reaction or by running polarization experiments. Only few studies elaborated on the combined effect caused by the use of MPL on the anode or cathode in an operating DMFC [19,28]. Hence, in this paper, the benefits of the anode GDL surface coated with MPL to the performance of an operating DMFC are studied. Regarding the polarization curves and the specific performance at various constant current densities, in situ EIS measurements, differing from conventional half cell impedance measurements, are utilized to resolve the anode and cathode impedance from the full cell impedance for the whole reaction. By adjusting the parameters of current density, methanol concentration, and air flow rate, the influences of the anode MPL on the anode and cathode reaction are respectively demonstrated. Furthermore, the results are compared with those of the MEA without anodic MPL, and then an analysis and discussion of the combined effect of MPL on the interaction between anode and cathode are offered systematically.

2. Experimental

2.1. Preparation of the membrane electrode assembly

The MEAs consisting of electrodes and the electrolyte membrane were prepared by the procedure reported in our previous work [29,30]. The catalysts were purchased form Johnson Matthey, Inc. The electrode inks were fabricated from a mixture of Nafion solution (DuPont) and Pt-Ru/C or Pt/C catalysts. A thin layer of electrode with this catalyst was then coated on each surface of the cleansed Nafion 117 membrane by a screen-printing technique. Pt–Ru and Pt were deposited onto the anode and cathode, respectively, both at a loading rate of 2 mg cm^{-2}. After hot-pressing at 120 °C and 50 kg cm^{-2} for 2 min, the active area of the MEA was aligned to 25 cm^2 using a laser-ablation process [31,32]. Two types of diffusion layers were used: (1) the hydrophobized carbon paper (SGL SIGRACET 10BA, 10 wt.% PTFE) and (2) the MPL-coated carbon paper (SGL SIGRACET 10BB, 10 wt.% PTFE). The MPL-coated woven carbon cloth (E-Tek LT 1400-W) was the only type of GDL used for the cathode side throughout the experimental program. The details of these GDL were listed in Table 1. The surface morphologies of the two different carbon papers were demonstrated in Fig. 1 by using the scanning electron microscopy (Hitachi S-4800 SEM,

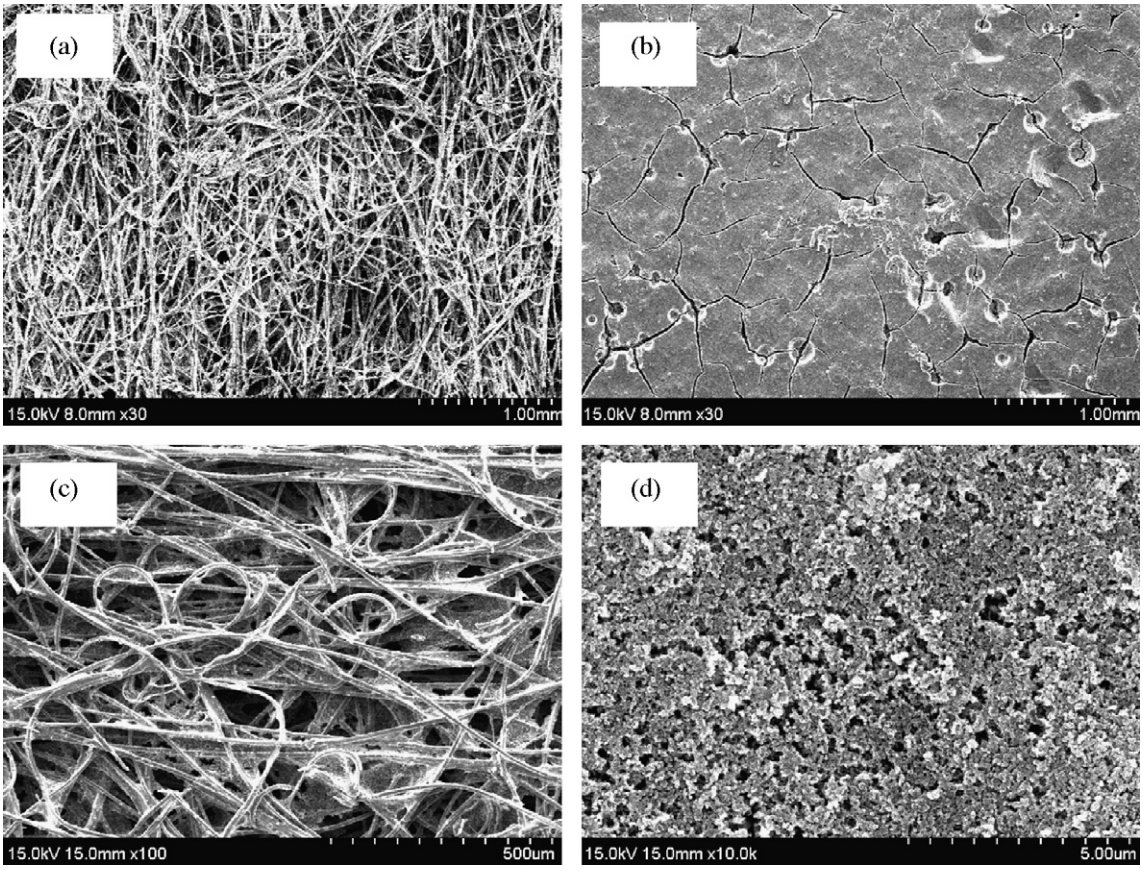

Fig. 1. SEM images of the hydrophobized carbon paper (a) 30×, (b) 100× and the MPL-coated carbon paper (a) 30×, (b) 10,000×.

Table 1
Properties of gas diffusion materials.

GDL	Thickness	Area weight	Porosity
SGL 10BA	402 μm	85 g m^{-2}	88.6
SGL 10BB	423 μm	125 g m^{-2}	84.2
E-Tek LT 1400-W	409 μm	210 g m^{-2}	83.1

Japan). The hydrophobized carbon paper was a microscopically complex fibrous structure (Fig. 1(a)) with the pore size distribution ranging from a few microns to twenties of microns (Fig. 1(b)). The MPL-coated carbon had uniform cracks (mud cracking), induced by volume shrinkage of carbon/PTFE slurry during annealing in Fig. 1(c) and provides a larger pore distribution due to much smaller pore size (~100 nm), as shown in Fig. 1(d). All gas diffusion materials were used for evaluation as received. There were two different MEAs prepared for the anode GDL evaluation in our experiment. One anode GDL was the MPL-coated carbon paper, and the other was the hydrophobized carbon paper without MPL. Subsequently, the MEA was installed in a test block with the current collectors positioned at each end and then sandwiched between gas-diffusion layers. The gasket thickness of both anode and cathode side was 0.3 mm. Channels with parallel geometry (1 mm wide, 1.2 mm deep, with ridges 1 mm high) were machined in the plates.

2.2. Operating conditions and electrochemical measurement

Before the test, the cell was preheated to 60 °C at the anode flow rate of 2 cm^3 min^{-1} for 1 h without air supply. Then, a load of 40 mA cm^{-2} was applied at the cathode flow of 100 ml min^{-1} for 1 h to insure a steady state. Testing was performed by a computer-controlled Medusa RD Fuel Cell Test station (Teledyne Energy Systems, Inc.) with a 50A/100W Model 890CL electronic load (Scribner Associates, Inc.) and Model 880 Frequency Response Analyzer (Scribner Associates, Inc.). Three methanol concentrations of 0.5, 1.0, and 2.0 M were used here. Both the methanol and air flows were load controlled to achieve the required stoichiometry at each test. For all impedance measurements, the range of measured frequencies was set from 1 kHz to 0.05 Hz with 10 steps per logarithmic decade. The amplitude of the sinusoidal modulation voltage did not exceed 10 mV. To resolve the anode and cathode impedance, an Ag/AgCl electrode (MF-2052, BAS Inc.) was placed at the region of constant potential (RCP) [32–36] of the membrane as a reference electrode. The detailed description of the setup of reference electrode was proposed and demonstrated in our previous work [32].

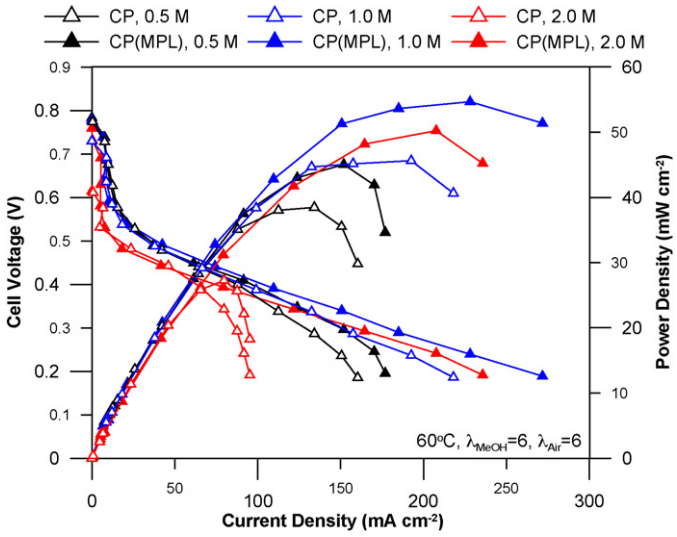

Fig. 2. Polarization curves of a DMFC with different anode GDLs under various methanol concentration. Cell temperature is 60 °C, both the air and methanol flow are 6-stoichiometry.

All the impedance spectra were measured under the galvanostatic mode.

3. Result and discussions

The polarization curves of the MEA with the different anode GDL at different concentrations of methanol solution (0.5, 1.0, and 2.0 M) were demonstrated in Fig. 2. Both the stoichiometric flow of methanol and air were set to six at a cell temperature of 60 °C. Obviously, the MEA which used a MPL-coated carbon paper as an anode GDL always presented a higher performance than that with the hydrophobized carbon paper on the anode side, especially in a high current density region with 2.0 M methanol. It is worth noting that the open circuit potential (OCP) of the MEA with anodic MPL did not vary with a change of methanol concentration. However, a continuous decrease of the OCP with increasing methanol concentration [15,37] was distinguished from the polarization test of the MEA without anodic MPL in Fig. 2. The results can be explained with that the MPL provided a barrier to methanol diffusion and thereby reduced methanol crossover [15,24]. Regarding the polarization curves, the short-term tests at a constant current density

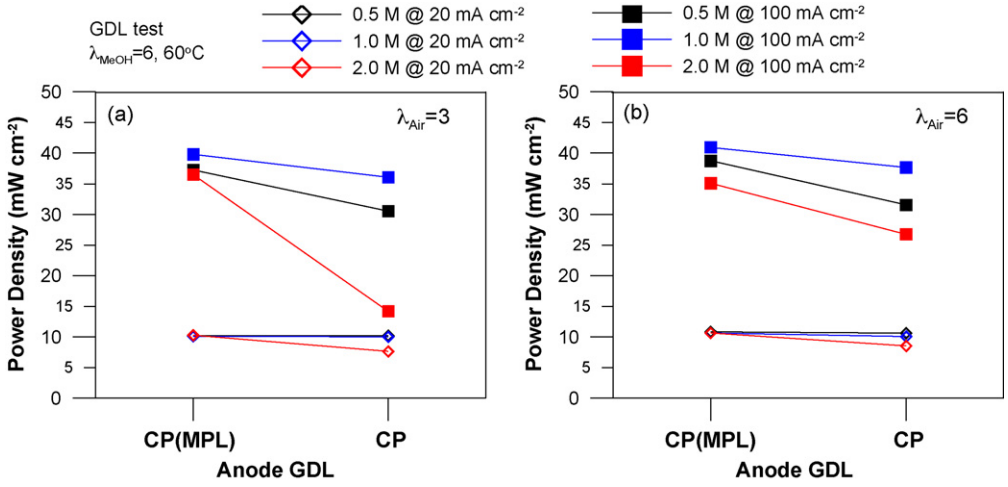

Fig. 3. Specific cell performance of a DMFC with different anode GDL under various methanol concentrations at air stoichiometric flow of (a) 3 and (b) 6. Cell temperature is 60 °C, methanol flow is 6-stoichiometry.

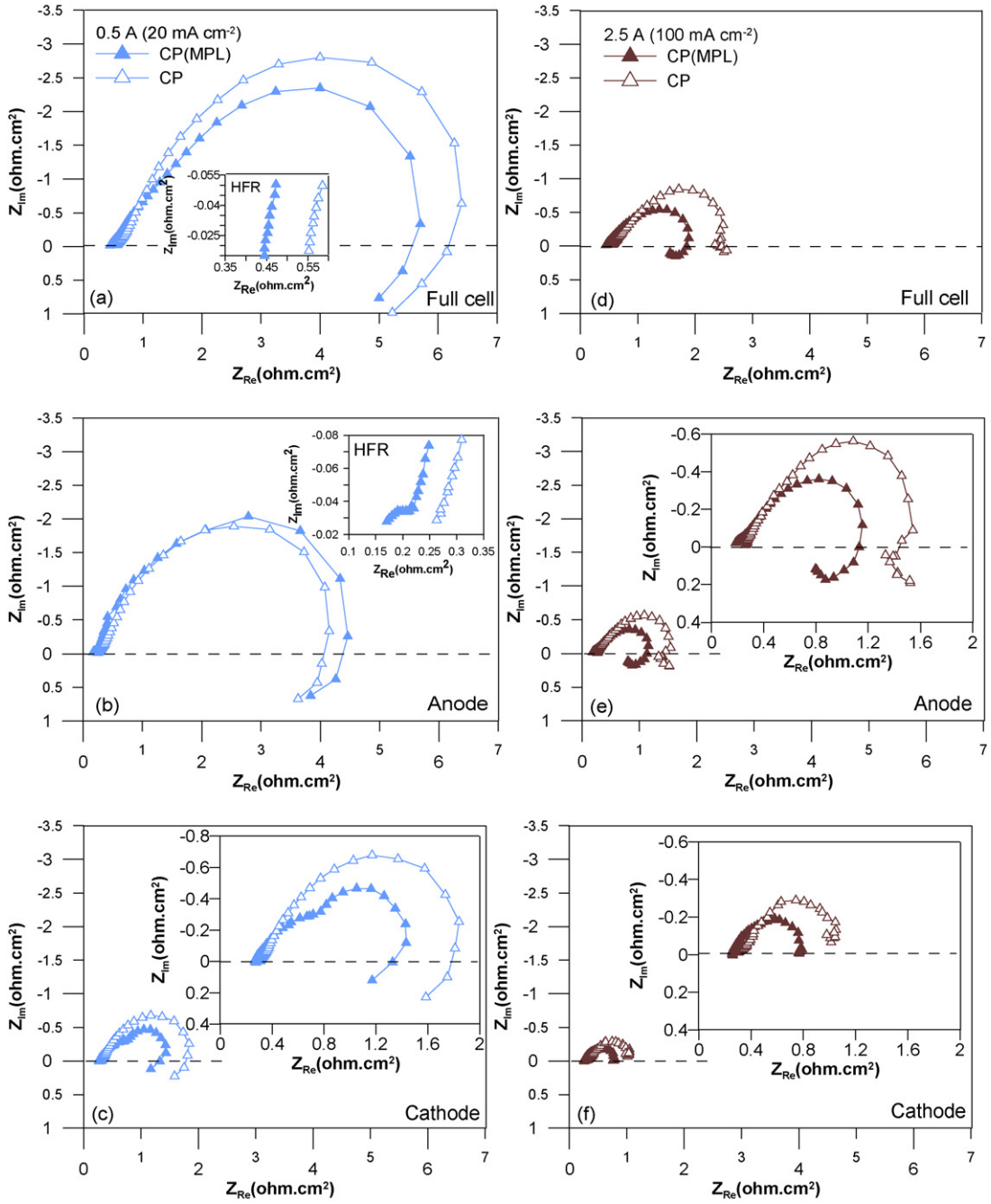

Fig. 4. Combined EIS measurements of a DMFC with different anode GDLs at 1.0 M methanol concentration: (a) full cell, (b) anode, and (c) cathode at 20 mA cm^{-2}, (d) full cell, (e) anode, and (f) cathode at 100 mA cm^{-2}. Cell temperature is 60 °C, both the air and methanol flow are 6-stoichiometry.

of 20 mA cm^{-2} and 100 mA cm^{-2} were carried out by varying the methanol concentration together with the air flow. The average power density of each short-term test between the two different MEAs under various operating conditions was shown in Fig. 3. At different methanol concentrations, the MEA with anodic MPL always performed a better performance than that without anodic MPL at a high current density of 100 mA cm^{-2}. However, no significant differences in performance between the two different MEAs were observed at a low current density of 20 mA cm^{-2}. Furthermore, at high current density and high methanol concentration, the variation in air flow had negligible influence on the performance of the MEA with anode MPL but clearly caused a performance drop of the MEA without anode MPL. According to the polarization curves or the specific performance at various constant current densities, it is difficult to interpret the influence of the anode MPL on the anode and whether cathode reaction was affected as well. Then, the in situ EIS measurements were used as a tool to observe the influences of the anode GDL with and without MPL on anode and cathode reactions based on various current densities, methanol concentrations and stoichiometric flows of air.

3.1. *Effect of operating current density*

After setting both the stoichiometric flow of air and 1.0 M methanol to 6, the in situ EIS of the anode, cathode and full cell of the two different MEA were simultaneously carried out. Taking the operation at a low current density of 20 mA cm^{-2} and a high current of 100 mA cm^{-2} into consideration, the EIS measure-

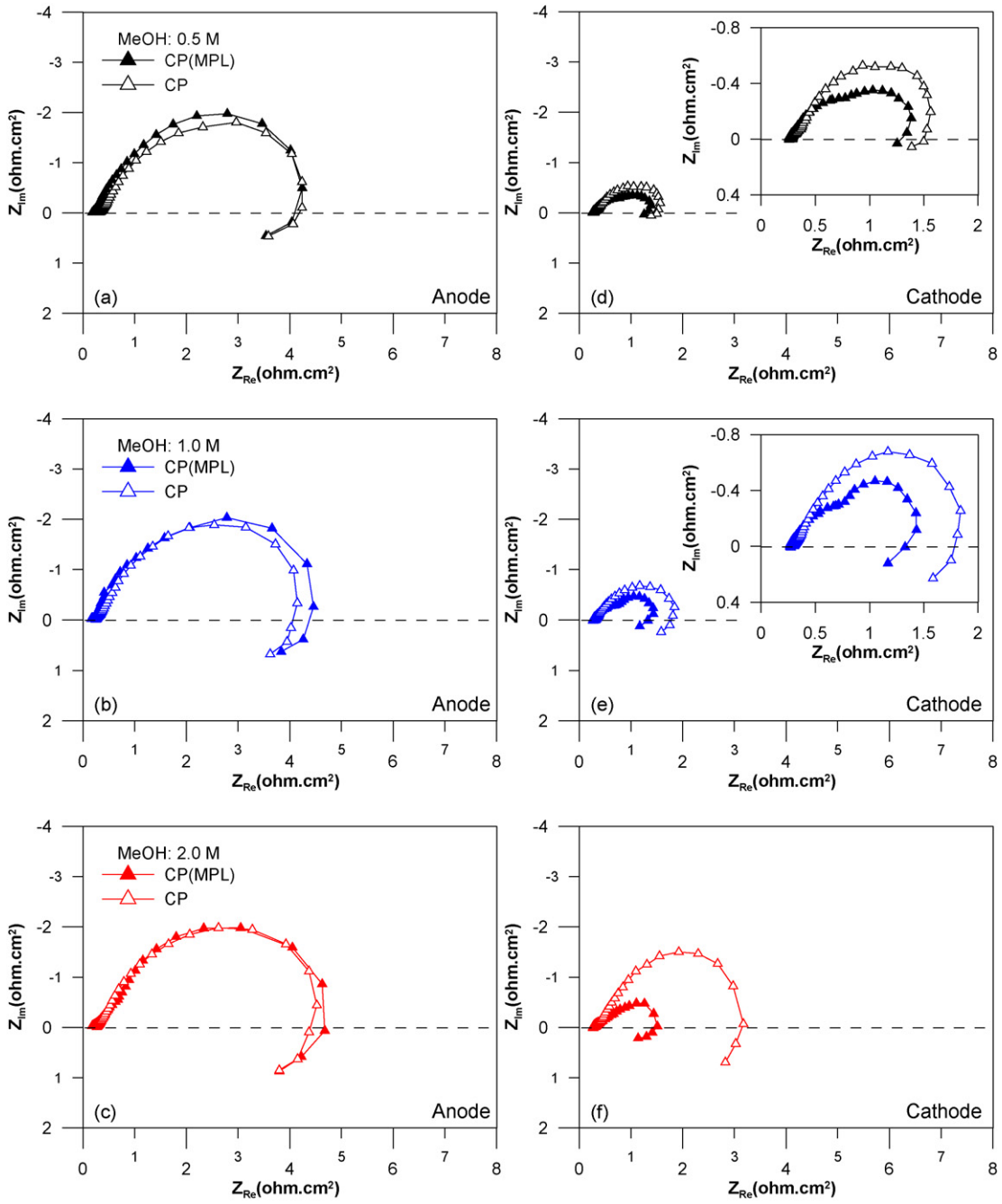

Fig. 5. Combined EIS measurements of a DMFC with different anode GDLs at 20 mA cm^{-2}: (a) anode and (d) cathode at 0.5 M methanol concentration. (b) Anode and (e) cathode at 1.0 M methanol concentration. (c) Anode and (f) cathode at 2.0 M methanol concentration. Cell temperature is 60 °C, both the air and methanol flow are 6-stoichiometry.

ments were demonstrated in Fig. 4. At a low current density of 20 mA cm^{-2}, the full cell impedance of the MEA with anodic MPL exhibited a lower high frequency resistance (HFR) and charge transfer resistance (CTR) than the MEA without anodic MPL. Dividing the full cell impedance into two parts, the in situ impedance of the anode and cathode were illustrated in Fig. 4(b) and (c), respectively. In Fig. 4(b), the MEA with anodic MPL presented a lower HFR of anode impedance since the MPL effectively reduced the contact resistance of the electrode [14,21,38–44]. However, due to a lower kinetics of MOR, no significant differences in the CTR of the anode impedance between the two types of MEA were observed. Corresponding to the anode EIS at a 1.0 M methanol concentration, the cathode EIS at a low current density of 20 mA cm^{-2} was shown in Fig. 4(c). Obviously, the MEA with anodic MPL had a lower CTR of cathode impedance than the one without MPL. This is because the thicker and lower porosity of anodic MPL, as listed in Table 1, effectively reduces the methanol permeation and water crossover [14,15,19,21–24]. Thus, the influence of methanol and water crossover on the cathode impedance of the MEA with anodic MPL was declined as compared with that of the MEA without anodic MPL. Nevertheless, the reduction of methanol and water crossover did not critically affect the cell performance at a low current density because of a slower kinetics.

When the current density was increased to 100 mA cm^{-2}, the kinetics of interaction of a DMFC was enhanced along with the charge transfer process [45–47]. Therefore, all the EIS results of the full cell, anode and cathode of the two MEA were smaller than the EIS measurements at 20 mA cm^{-2} as compared in

Figs. 3(d–f) and 4(a–c). In the anode reaction, Fig. 4(e) shows that the anode impedance of the MEA with anodic MPL not only exhibited a lower HFR but also presented a lower CTR than the one without anodic MPL. This is because that the MPL structure provided a larger pore distribution than the hydrophobized carbon paper in Fig. 1 and then results in more uniform transportation of gas and solution due to a large pore distribution [16,19]. Furthermore, the carbon surface hydrophobicity resulting from PTFE created more regions for the gas removal, which accelerated the ejection of CO_2 from the catalyst surface into the fluid channel [22]. As a result, the anode catalyst utilization efficiency was increased and so was the kinetics of the methanol oxidation reaction (MOR) [6–8,10,12,18]. Thus, the MEA with anodic MPL presented a lower CTR of anode impedance. However, the use of carbon paper without MPL led more CO_2 bubbles or slugs to cover the catalyst surface and then enhanced the diffusion resistance of the two phase transport [5–7,13,18]. Thereby, the depressed MOR caused a higher CTR of anode impedance spectrum at low frequency, as shown in Fig. 4(e). On the cathode side, increasing the current density reduced the flux of methanol crossover and water permeation [5,21]. Obviously, Fig. 4(f) shows that the use of MPL-coated carbon paper performed a smaller cathode impedance arc than that of hydrophobized carbon paper. This result could be explained with the combined effect of each electrode in DMFCs [28,32,46]. Since the MPL-coated carbon paper yielded the faster kinetics of MOR, the sufficient protons and electrons transported fast to cathode side. Therefore, the kinetics of cathode oxygen reduction reaction (ORR) was reinforced together with the increased kinetics of MOR in the whole reaction by using of the MPL-coated anode GDL.

3.2. Effect of methanol concentration

Taking the influence of methanol concentrations into consideration, the in situ EIS of the full cell, anode and cathode of the two different MEA were carried out at different current densities of 20 mA cm^{-2} and 100 mA cm^{-2}. At a low current density of 20 mA cm^{-2}, a comparison of anode EIS in Fig. 5(a–c) shows that both the two different MEAs revealed an increase of CTR and inductive parts in a low frequency region. This is because the intermediate adsorption quantity of CO on the anode catalyst surface varies with a change of methanol concentration [8,37,38]. Notably, at a same methanol concentration, no obvious variation in the anode EIS between the two different MEAs are observed even if the methanol concentration was increased to 2.0 M. This result reveals that the MPL structure did not benefit the anode reaction at a low current density. Nevertheless, the comparisons of different cathode EIS in Fig. 5(d)–(f) indicate that the different anode GDLs of MEA resulted in a clear variation in cathode impedance especially at a high methanol concentration of 2.0 M. The result could be interpreted in light of the efficiency of MPL to reduce the methanol crossover as mentioned above. Therefore, increasing methanol concentration yielded minor effects on the cathode impedance of the MEA with anodic MPL, as displayed in Fig. 5(d–f). In contrast with the MEA with anodic MPL, the use of carbon paper as anode GDL caused a violent change in both the CTR and inductive parts of the cathode impedance by increasing the methanol concentration. This is because the use of carbon paper could not efficiently decrease the methanol permeation into cathode side and thereby decreased the kinetics of ORR with increasing methanol concentration [21]. Regarding the in situ EIS of each electrode, it is worth of noticing that although the methanol concentration was up to 2.0 M, the coating MPL on anode GDL seemed to have no effect on the anode reaction at a low current density except for the reduction of the contact resistance of the electrode. However, the effective fuel management of the anodic MPL could reduce the influence of methanol crossover on the cathode ORR so that the MEA with the anodic MPL presented the minor variations in the cathode EIS with changing methanol concentrations, as shown in Fig. 5(d–f). As a result, in the whole reaction, Fig. 6 shows that the variations in the full cell impedance of the MEA with anodic MPL caused by different methanol concentrations was smaller than that of the MEA without anodic MPL.

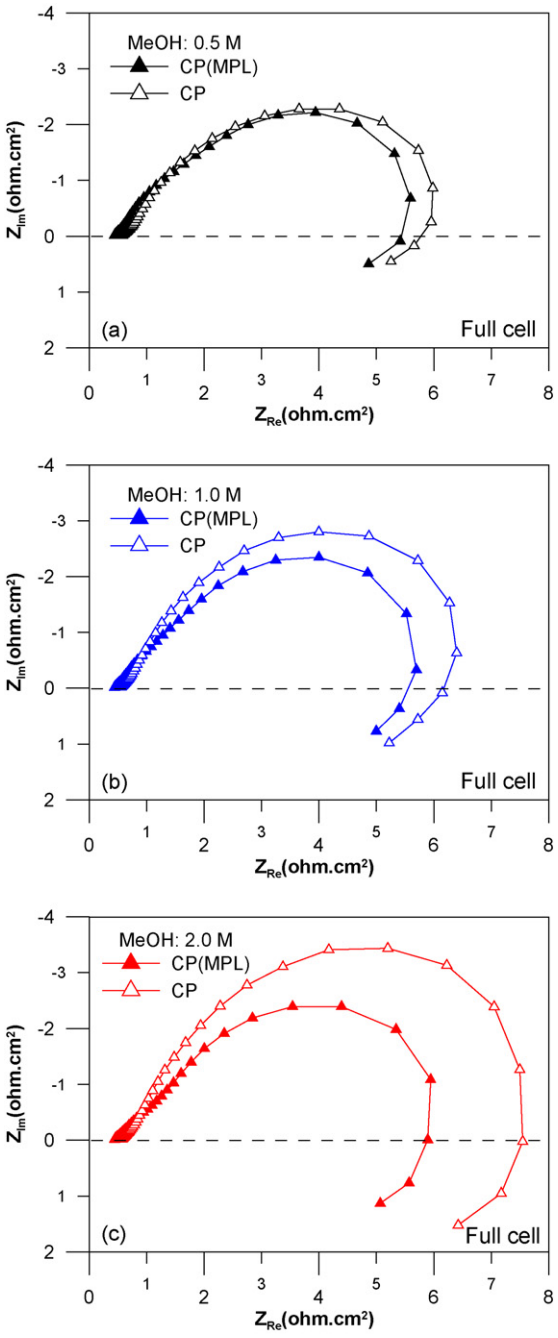

Fig. 6. Full cell EIS of a DMFC with different anode GDLs at 20 mA cm^{-2} and various methanol concentrations: (a) 0.5 M, (b) 1.0 M, and (c) 2.0 M. Cell temperature is 60 °C, both the air and methanol flow are 6-stoichiometry.

At a high current density of 100 mA cm^{-2}, the use of 0.5 M methanol yielded the significant concentration polarization, reducing the kinetics of the MOR [37,48,49]. Hence, both the two MEAs presented a large anode EIS arc with visible mass transport problems in a low frequency region, as shown in Fig. 7(a). Notably, the MEA with anodic MPL still illustrated smaller anode impedance than that of the MEA without anodic MPL. This is because the MPL

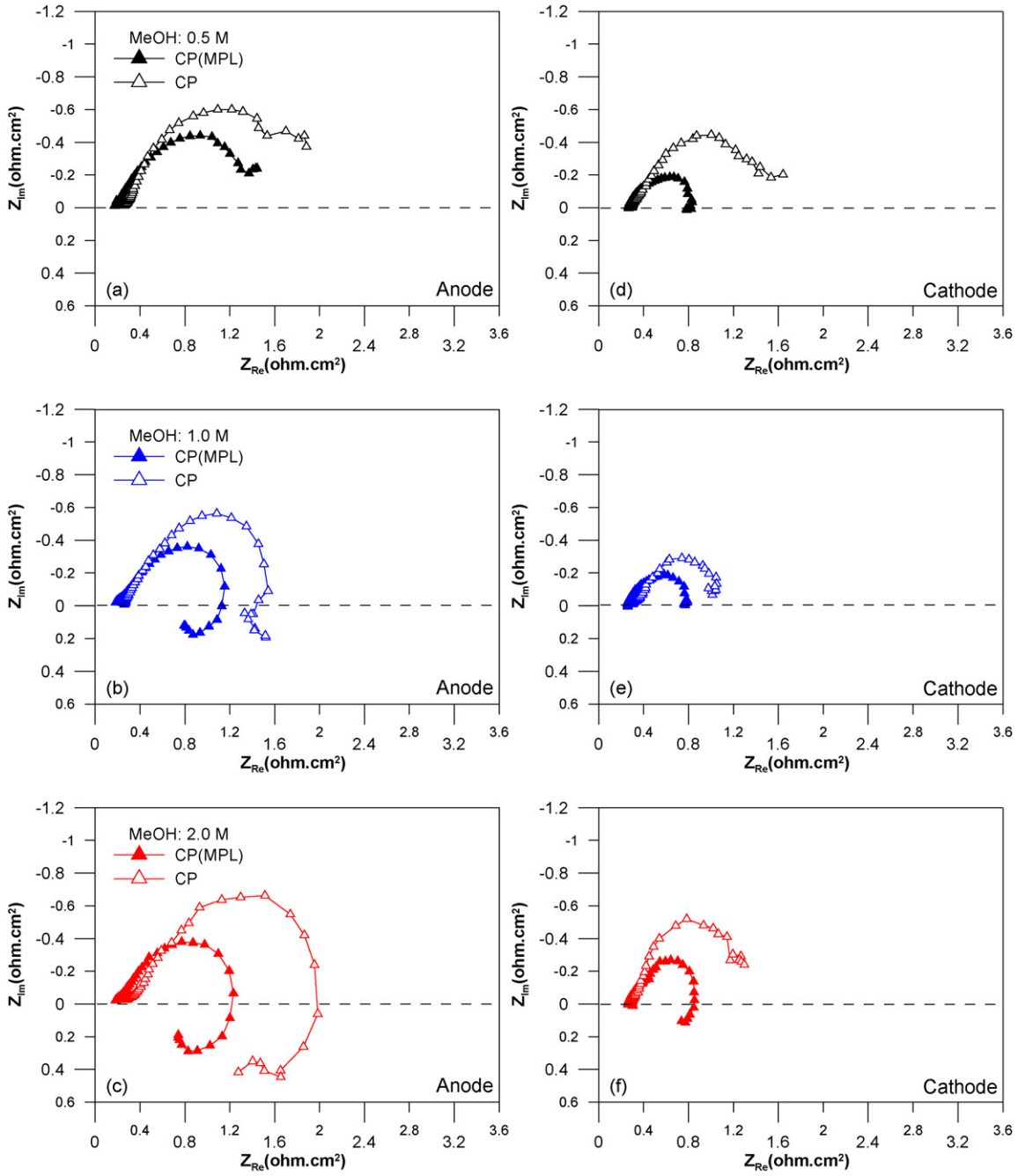

Fig. 7. Combined EIS measurements of a DMFC with different anode GDLs at 100 mA cm^{-2}: (a) anode and (d) cathode at 0.5 M methanol concentration. (b) Anode and (e) cathode at 1.0 M methanol concentration. (c) Anode and (f) cathode at 2.0 M methanol concentration. Cell temperature is 60 °C, both the air and methanol flow are 6-stoichiometry.

structure provided a higher utilization efficiency of anode catalyst due to a faster CO_2 gas removal and thereby enhanced the kinetics of MOR. Meanwhile, the more protons and electrons transported into cathode, yielding the faster kinetics of ORR. Therefore, Fig. 7(d) shows that the MEA with anodic MPL presented a smaller cathode EIS than that of the MEA without anodic MPL. However, the use of carbon paper as anode GDL lowered the kinetics of the anode MOR because slower gas removal strengthened the mass transfer limitations caused by the low methanol concentration. With the reduction of the kinetics of the anode MOR, the kinetics of the cathode ORR were depressed as well. Therefore, in contrast with the EIS of the MEA with anodic MPL, both the EIS of anode and cathode in the MEA without anodic MPL presented a larger impedance arc with a low frequency irregular shape, as illustrated in Fig. 7(a) and (d). By increasing the methanol concentration to 1.0 M, Fig. 7(b) shows that both the two MEAs revealed the elimination of the low frequency irregular parts in the anode impedance because of the reduction of mass transport limitations. However, the slower two phase transport caused by the use of carbon paper still limited the anode MOR and then depressed the cathode ORR in the whole reaction. Consequently, both the EIS of the anode and cathode in the MEA, lacking anodic MPL, had a larger diameter than that of the MEA with anodic MPL, as respectively displayed Fig. 7(b) and (e). When the methanol concentration was increased to 2.0 M, the intermediate adsorption of CO on the anode catalyst surface was increased as well [8,37,38,49]. However, the anode impedance of the MEA with anodic MPL at 2.0 M methanol (see Fig. 7(c)) was similar to the one at 1.0 M methanol (see Fig. 7(b)). It can be explained

with a less intermediate adsorption of CO on the anode catalyst surface as more CO became CO_2 and then was fast transported to the fuel channel. However, the slower gas removal of the anode GDL led a more amount of CO to adsorb on the anode catalyst surface, reducing the active area of the catalyst [6,7,10,13,18,37,48]. Therefore, a comparison between Fig. 7(b) and (c) clearly indicates that increasing methanol concentration yielded the obvious increase of both CTR and inductive parts of the anode impedance in the MEA without anodic MPL. Taking the cathode reaction into consideration, the comparison of cathode EIS between Fig. 7(e) and (f) indicates that increasing methanol concentration from 1.0 to 2.0 M only induced a minor effect on the cathode impedance of the MEA with anodic MPL. This is because the influence of the methanol crossover on the cathode ORR was reduced by the anodic MPL. However, the use of hydrophobized carbon paper could not effectively restrict the methanol crossover to the cathode side so that the active area of the cathode catalyst was decreased together with the kinetics of the ORR at a high methanol concentration. Meanwhile, the methanol was oxidized in the cathode by consuming oxygen, resulting in the influence of the oxygen mass transport limitation on the ORR. Hence, as compared with Fig. 7(e) and (f) shows that the MEA, which lacks the anodic MPL, revealed the obvious growth of the cathode impedance within the irregular shape in the low frequency region by increasing the methanol concentration from 1.0 to 2.0 M.

In Fig. 8, the resultant effect of both anode and cathode on the overall reaction was plotted in the form of full cell impedance. According to the separated EIS of each electrode, using MPL-coated anode GDL provided higher catalyst utilization, effectively promoting the stability and kinetics of anode MOR. Simultaneously, the anode MPL structure reduced the flux of methanol crossover, securing the kinetics of cathode ORR. Consequently, although the methanol concentration was changed, the MEA with anodic MPL always performed a fast and stable kinetics of both the MOR and ORR. Thereby, a comparison between Fig. 8(a)–(c) indicates that the deviation of the full cell EIS caused by changing the methanol concentration in the MEA with anodic MPL was not as sharp as that in the MEA without anodic MPL.

3.3. Effect of air flow

Two air flow rates, corresponding to cathode stoichiometric coefficients of 3 and 6, were set for the two MEAs. A comparison between Fig. 3(a) and (b) indicated the indistinct influence of changing air flow on the cell performance (100 mA cm^{-2}) at both 0.5 and 1.0 M methanol concentration, whether the MPL had been coated on the anode GDL or not. As the methanol concentration increased to 2.0 M, the variation of air flow still resulted in a minor effect on the performance of the MEA with anodic MPL but yielded a sharp performance drop of the MEA without anodic MPL. However, this phenomenon did not occur at a low current density of 20 mA cm^{-2}.

To clarify the influence of changing air flow on the performance of the two MEAs, the in situ EIS measurement under a constant current density of 100 mA cm^{-2} were carried out at 1.0 and 2.0 M methanol, as demonstrated in Fig. 9. At a methanol concentration of 1.0 M, the influences of various cathode air flows on both the MOR and ORR of each MEA were obscure, although the use of anode GDL was different. Thus, not only the MEA with anodic MPL but also the one without anodic MPL revealed the imperceptible changes of both anode and cathode impedance at different air flows, as plotted in Fig. 9(a) and (b), respectively. This is because the stoichiometric air flow of 3 had provided sufficient oxygen concentration for the cathode ORR together with stable water ejection of the cathode flow channel. Hence, the kinetics of the anode MOR, corresponding to the stable ORR of the cathode, became steady as well [32].

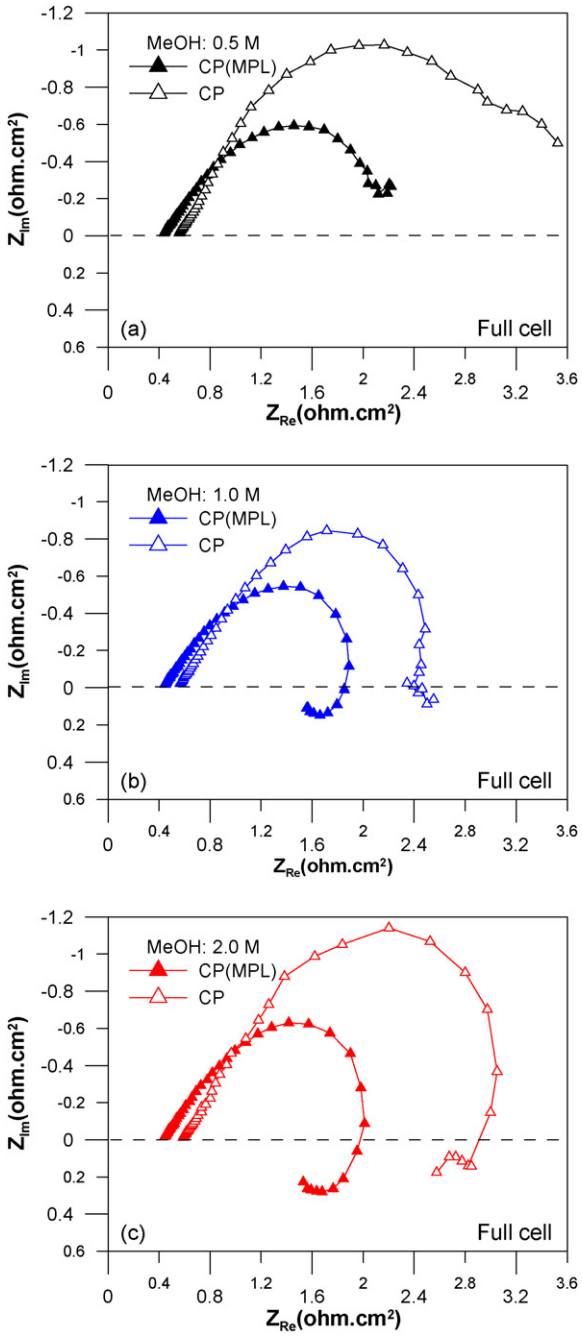

Fig. 8. Full cell EIS of a DMFC with different anode GDLs at 100 mA cm^{-2} and various methanol concentrations: (a) 0.5 M, (b) 1.0 M, and (c) 2.0 M. Cell temperature is 60 °C, both the air and methanol flow are 6-stoichiometry.

Since the stoichiometric air flow was up to 6, both the two MEAs presented minor changes in the low frequency region of the anode and cathode impedance spectra. It can be concluded that a change of air flow stoichiometric coefficient slightly accelerated the oxygen mass transport together with the water removal and thereby slightly affected the cathode ORR along with the anode MOR. Owing to the illegible variations in the anode and cathode EIS of each MEA, caused by the different air stoichiometric coefficients, Fig. 9(c) presented no significant deviations in the full cell impedance of each MEA at various cathode air flow, whether the MEA equipped with the anodic MPL or not. The results just corresponded to the difference in performance of each MEA at 100 mA cm^{-2} between air stoichiometric flows of 3 and 6, as plotted in Fig. 3(a) and (b).

At a methanol concentration of 2.0 M, a change in the air stoichiometric coefficient obviously affected both the real-time anode and cathode impedance of the MEA without anodic MPL, as illustrated in Fig. 9(d) and (e). This is because the use of the hydrophobized carbon paper induced the methanol crossover so that the effective active area of the cathode catalyst as well as the oxygen concentration was reduced on the cathode side. By decreasing the air stoichiometry coefficient from 6 to 3 in our work, the oxygen concentration and the methanol removal on the cathode side decreased as well. Therefore, the mass transport limitations critically reduced the kinetics of the ORR so that the MEA with the hydrophobized carbon paper revealed a larger arc of cathode impedance in Fig. 9(d). Meanwhile, Fig. 9(e) shows that a mixed potential slowed the transport of protons from the anode to cathode, yielding a sharp growth of the anode impedance. In contrast with the EIS of the MEA without anodic MPL, the MEA with anodic MPL performed similar cathode impedance by changing the air flow at 2.0 M methanol, as demonstrated in Fig. 9(d). Corresponding to the cathode EIS in Fig. 9(d), no obvious variation in the anode impedance was observed with the different air stoichiometric coefficients, as displayed in Fig. 9(e). This is because the MPL-coated GDL effectively reduced the methanol crossover so that the protons transferred from the anode would stably react with sufficient oxygen at the cathode side.

According to the above mentioned in situ EIS of each electrode, it can be concluded that a methanol crossover was the prime agent of the variation in both the anode and cathode reaction for the various air stoichiometric coefficients. Since the MPL on the anode

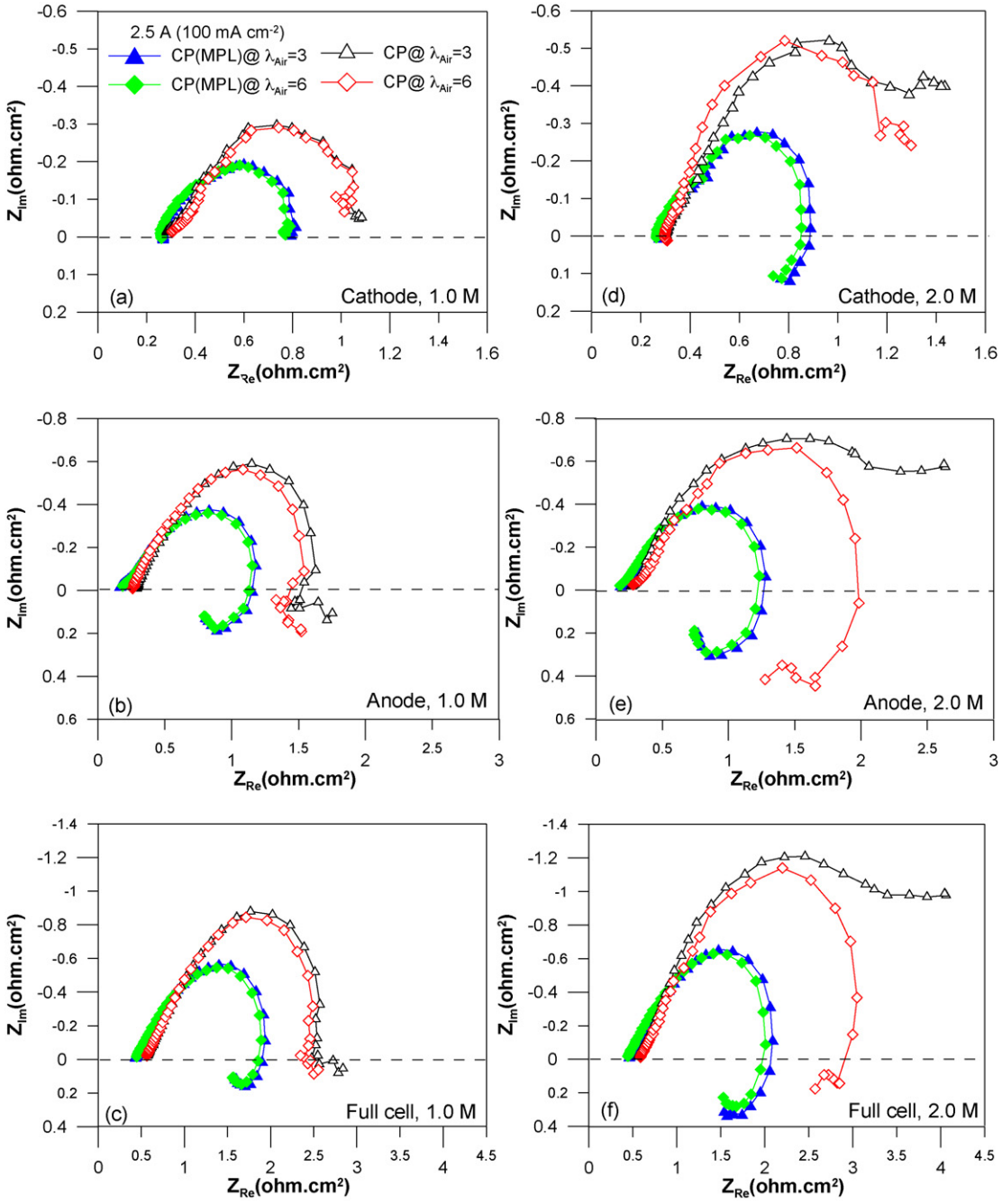

Fig. 9. Combined EIS of a DMFC with different anode GDL at 100 mA cm^{-2} under various air flow rates: (a) full cell, (b) cathode, and (c) anode at 1.0 M methanol. (d) Full cell, (e) cathode, and (f) anode at 2.0 M methanol.

GDL acted as a barrier against the methanol crossover at a high methanol concentration, a change of air flow resulted in a minor influence on both the MOR and ORR in the whole reaction. Consequently, Fig. 9(f) shows that no momentous variations in the full cell impedance of the MEA with anodic MPL had been observed at 2.0 M methanol with the air stoichiometric coefficient. However, using the hydrophobized carbon paper caused the methanol crossover, critically affecting both the MOR and ORR of a DMFC with a change of the air stoichiometry coefficient. Therefore, given the sharp drop of cell performance at 100 mA cm^{-2} caused by the various air flows (see Fig. 3(a) and (b)), Fig. 9(f) shows that the full cell impedance of the MEA without anodic MPL varied violently with the air stoichiometry coefficient.

4. Conclusions

In this paper, the advantages of the use of a MPL-coated anode GDL for an operating direct methanol fuel cell (DMFC) are studied. Taking into account the operating conditions such as the current density, methanol concentration and air stoichiometric flow, a comparison between the MEA with and without anodic MPL was systematically carried out by measuring the polarization curves and specific performance at various constant current densities. Corresponding to the polarization curves and specific performance, the in situ EIS measurement indicates that coating MPL on the anode GDL effectively accelerates the kinetics of the anode reaction together with the kinetics of the cathode reaction. Therefore, at a high current density of 100 mA cm^{-2}, the performance of the MEA with anodic MPL is obviously better than that without anodic MPL. The conclusions are summarized as follows:

1. Since the carbon powder of the MPL effectively reduces the contact resistance of the electrode surface, the MEA with anodic MPL exhibits a lower HFR of the anode impedance as well as a lower HFR of the full cell impedance.
2. At a high current density of 100 mA cm^{-2}, the use of the MPL-coated anode GDL performs better with MEA than a bare anode GDL. This is because the carbon surface is hydrophobic, and the greater micro-pore distribution of MPL accelerates the two phase transport, improving the kinetics of the anode MOR together with the cathode ORR. However, at a low current density of 20 mA cm^{-2}, the effects resulting from the production of CO_2, ohmic losses and methanol crossover on cell performance can be eliminated by slower kinetics. Therefore, the influence of the anode MPL on the MEA performance at 20 mA cm^{-2} is not as obvious as that at 100 mA cm^{-2} even though the in situ EIS measurement clearly reveals the decrease of the methanol crossover due to the anodic MPL.
3. Coating MPL on the anode GDL not only provides a greater pore distribution to lower the mass transport limitations at a low methanol concentration but also effectively manages the transport of methanol for the anode electrode to reduce the methanol crossover at a high methanol concentration. As a result, the MEA with anodic MPL yields the faster MOR and ORR, generating higher and more stable cell performance at a high current density with a change of methanol concentration.
4. According to the in situ EIS, the influence of methanol crossover is the prime agent of both the anode and cathode reactions, which vary with the changing air stoichiometry coefficient (from 6 to 3 in this paper). By using the MPL-coated anode GDL, the physical properties of MPL effectively decrease the influence of the methanol crossover and maintain the stability of both the MOR and ORR as well. Therefore, the performance of the MEA with anodic MPL does not critically vary with the air stoichiometry coefficient at a high methanol concentration.

According to the conclusions, the influences of the MPL on the performance of a DMFC during actual operation have been clearly studied. In our future work, the advantages of MPL will be employed to improve the performance and durability of fuel cells and finally to facilitate the commercialization of full cells.

Acknowledgement

The authors would like to thank the institute of Nuclear Energy Research (INER) for financially supporting this research.

References

[1] A.S. Arico, S. Srinivasan, V. Antonucci, Fuel Cells 1 (2001) 133.
[2] X. Cheng, C. Peng, M. You, L. Liu, Y. Zhang, Q. Fan, Electrochim. Acta 51 (2006) 4620.
[3] P. Piela, C. Eikes, E. Brosha, F. Garzon, P. Zelenay, J. Electrochem. Soc. 151 (2004) A2053.
[4] K. Scott, W. Taama, J. Cruickshank, J. Appl. Electrochem. 28 (1998) 289.
[5] V. gogel, T. Frey, Z. Yongsheng, K.A. Friedrich, L. Jorissen, J. Garche, J. Power Sources 127 (2004) 172.
[6] K. Scott, W.M. Taama, P. Argyropoulos, J. Appl. Electrochem. 28 (1998) 1389.
[7] K. Scott, W.M. Taama, P. Argyropoulos, J. Power Sources 79 (1999) 43.
[8] A. Oedegaard, C. Hebling, A. Schmitz, S. Moller-Holst, R. Tunold, J. Power Sources 127 (2004) 187.
[9] S. Arisetty, A.K. Prasad, S.G. Advani, J. Power Sources 165 (2007) 49.
[10] Q. Liao, X. Zhu, X. Zheng, Y. Ding, J. Power Sources 171 (2007) 644.
[11] J. Zhang, G. Yin, Z. Wang, Y. Shao, J. Power Sources 160 (2006) 1035.
[12] J. Nordlund, A. Roessler, G. Lindbergh, J. Appl. Electrochem. 32 (2002) 259.
[13] K.T. Park, U.h. Jung, S.U. Jeong, S.H. Kim, J. Power Sources 162 (2006) 192.
[14] J. Zhang, G.P. Yin, Q.Z. Lai, Z.B. Wang, K.D. Cai, P. Liu, J. Power Sources 168 (2007) 453.
[15] N. Wan, Z. Mao, C. Wang, G. Wang, J. Power Sources 163 (2007) 725.
[16] C. Xu, T.S. Zhao, Q. Ye, Electrochim. Acta 51 (2006) 5524.
[17] L. Jianguo, S. Gongquan, Z. Fengliang, W. Guoxiong, Z. Gang, C. Likang, Y. Baolian, X. Qin, J. Power Sources 133 (2004) 175.
[18] A. Linedermeir, G. Rosenthal, U. Kunz, U. Hoffmann, J. Power Sources 129 (2004) 180.
[19] T.S. zhao, C. Xu, R. Chen, W.W. Yang, Prog. Energy Combust. Sci. 35 (2009) 275.
[20] M. Neergat, A.K. Shukla, J. Power Sources 104 (2002) 289.
[21] J.Y. Park, J.H. Lee, S.K. Kang, J.H. Sauk, I. Song, J. Power Sources 178 (2008) 181.
[22] Q.X. Wu, T.S. Zhao, R. Chen, W.W. Yang, J. Power Sources 191 (2009) 304.
[23] F Liu, C.Y. Wang, Electrochim. Acta 53 (2008) 5517.
[24] F. Liu, G. Lu, C.Y. Wang, J. Electrochem. Soc. 153 (2006) A543.
[25] J. Noedlund, A. Roessler, G. Lindbergh, J. Appl. Electrochem. 32 (2002) 259.
[26] Z.G. Shao, W.F. Lin, F. Zhu, P.A. Christensen, M. Li, H. Zhang, Electrochem. Commun. 8 (2006) 5.
[27] K.W. Park, B.K. Kwon, J.H. Choi, I.S. Park, Y.-M. Kim, Y.-E. Sung, J. Power Sources 109 (2002) 439.
[28] H.F. Zhang, S.Y. Wang, P.C. Pei, L. Chen, J.L. Li, X.D. Wang, Q.F. Li, Electrochem. Commun. 10 (2008) 407.
[29] C.Y. Chen, P. Yang, Y.S. Lee, K.F. Lin, J. Power Sources 141 (2005) 24.
[30] C.Y. Chen, C.S. Tsao, Int. J. Hydrogen Energy 31 (2006) 391.
[31] S. Eccarius, T. Manurung, C. Ziegler, J. Electrochem. Soc. 154 (2007) B852.
[32] S.H. Yang, C.Y. Chen, W.J. Wang, J. Power Sources, accept. http://dx.doi.org/10.1016/j.jpowsour.2009.10.066.
[33] S.H. Uhm, S.T. Chung, J.Y. Lee, J. Power Sources 178 (2008) 34.
[34] P. Piela, T.E. Springer, J. Davey, P. Zelenay, J. Phys. Chem. C 111 (2007) 6512.
[35] Z. Liu, J.S. Wainright, W. Haung, R.F. Sacinell, Electrochim. Acta 49 (2004) 923.
[36] X. Zhao, G. Sun, L. Jiang, W. Chen, S. Tang, Q. Xin, Electrochem. Solid-state Lett. 8 (2005) A149.
[37] J. Lobato, P. Cañizares, M.A. Rodrigo, J.J. Linares, A.F. Fragua, Chem. Eng. Sci. 61 (2006) 4773.
[38] G. Lin, T.V. Nguyen, J. Electrochem. Soc. 152 (2005) A1942.
[39] Z. Qi, A. Ksufmsn, J. Power Sources 109 (2002) 38.
[40] J.H. Nam, M. Kaviany, Int. J. Heat Mass Transfer 46 (2003) 4595.
[41] U. Pasaogullari, C.Y. Wang, Electrochim. Acta 49 (2004) 4359.
[42] G.G. Park, Y.J. Sohn, T.H. Yang, Y.G. Yoon, W.Y. Lee, C.S. Kim, J. Power Sources 131 (2004) 182.
[43] A. Weber, J. Newman, J. Electrochem. Soc. 152 (2005) A677.
[44] M.V. Williams, E. Begg, L. Bonville, H.R. Kunz, J.M. Fenton, J. Electrochem. Soc. 151 (2004) A1173.
[45] N.Y. Hsu, S.C. Yen, K.T. Jeng, C.C. Chen, J. Power Sources 161 (2006) 232.
[46] J.H. Liu, M.K. Jeon, W.C. Choi, S.I. Woo, J. Power Sources 137 (2004) 222.
[47] C.Y. Du, T.S. Zhao, W.W. Yang, Electrochim. Acta 52 (2007) 5266.
[48] D. Chakraborty, I. Chorkendorff, T. Johannessen, J. Power Sources 162 (2006) 1010.
[49] A. Oedegaard, J. Power Sources 157 (2006) 244.